

Topological crystalline semimetals in nonsymmorphic lattices

Yige Chen,¹ Heung-Sik Kim,¹ and Hae-Young Kee^{1,2,*}

¹*Department of Physics, University of Toronto, Ontario M5S 1A7, Canada*

²*Canadian Institute for Advanced Research, CIFAR Program in Quantum Materials, Toronto, ON M5G 1Z8, Canada*

(Received 25 January 2016; revised manuscript received 7 April 2016; published 21 April 2016)

Numerous efforts have been devoted to reveal exotic semimetallic phases with topologically nontrivial bulk and/or surface states in materials with strong spin-orbit coupling. In particular, semimetals with nodal line Fermi surface (FS) exhibit novel properties, and searching for candidate materials becomes an interesting research direction. Here we provide a generic condition for a fourfold degenerate nodal line FS in nonsymmorphic crystals with inversion and time-reversal symmetry (TRS). When there are two glide planes or screw axes perpendicular to each other, a pair of Bloch bands related by nonsymmorphic symmetry become degenerate on a Brillouin zone (BZ) boundary. There are two pairs of such bands, and they disperse in a way that the partners of two pairs are exchanged on other BZ boundaries. This enforces a nodal line FS on a BZ boundary plane protected by nonsymmorphic symmetries. When TRS is broken, fourfold degenerate Dirac points or Weyl ring FS could occur depending on a direction of the magnetic field. On a certain surface double helical surface states exist, which become double Fermi arcs as TRS is broken.

DOI: [10.1103/PhysRevB.93.155140](https://doi.org/10.1103/PhysRevB.93.155140)

I. INTRODUCTION

Recently intense interest has been drawn to novel topological semimetallic phases, in which the systems support nontrivial band crossing points in crystal momentum space. Such studies have been motivated by the discovery of topological insulators with a bulk energy gap and conducting surface modes protected by time-reversal symmetry (TRS) [1–11]. A list of topological semimetals, which is an extension of topological insulators to metallic phases, has been growing in theoretical communities, and some members in the list have been experimentally confirmed [12–15]. One group of topological semimetals is characterized by the Fermi surface (FS) points. This includes Weyl semimetals with chiral fermions [16–20], and three-dimensional (3D) Dirac semimetals with surface Fermi arc states [21–23]. Another class of topological semimetals is characterized by a closed loop of the FS called nodal line FS [24,25,27–31,35–37]. These semimetals named topological nodal line semimetals have recently been proposed in various materials, including a three-dimensional graphene network [29], Ca_3P_2 [32], Cu_3PdN [33], and orthorhombic perovskite iridates [24,31]. However, in graphene, Ca_3P_2 , and Cu_3PdN , spin-orbit coupling gaps out the nodal FS, and the system becomes a trivial insulator [37]. On the other hand, in perovskite iridates, spin-orbit coupling assists the system to develop a nodal line FS [24].

In this work, we provide a generic condition for a fourfold degenerate nodal line FS for three-dimensional spin (or pseudospin)-1/2 systems, where the nonsymmorphic crystal symmetry plays a critical role. In the presence of space-time inversion symmetry, all Bloch states are doubly degenerate due to the Kramers theorem. We show that when there are two glide planes or screw axes perpendicular to each other, two Bloch bands related by these operations form a degenerate pair on a BZ boundary. Their Kramers partners follow the same pattern, and thus four Bloch states are degenerate on a BZ boundary.

Due to the two nonsymmorphic symmetry operations, two pairs of such bands exist, and their partners within each pair should be exchanged when the Bloch bands disperse from one BZ boundary to another. This enforces a fourfold degenerate nodal line FS protected by nonsymmorphic symmetries on a BZ boundary plane. Using a tight binding model derived for perovskite iridates AIrO_3 (A being alkali earth elements) [24], we further show how a Dirac point or line of Weyl FS appears when TRS is broken. Surface states of this topological *crystalline* semimetal with and without TRS are also presented.

II. A SUFFICIENT CONDITION FOR NODAL-LINE SEMIMETAL WITH TRS

First, we provide a generic condition for a fourfold degenerate nodal line FS as shown in Fig. 1(a): a combination of two perpendicular nonsymmorphic symmetry operations together with space-time inversion symmetry guarantees a fourfold degenerate nodal line FS for a three-dimensional spin (pseudospin)-1/2 system. Let us consider the \hat{a} - and \hat{b} -axis twofold screw operators that are perpendicular to each other. The explicit form of those operations are given as follows:

$$\hat{S}_a : (x, y, z, t) \rightarrow \left(\frac{1}{2} + x, \frac{1}{2} - y, -z, t\right) \times i\hat{\sigma}_x, \quad (1)$$

$$\hat{S}_b : (x, y, z, t) \rightarrow \left(\frac{1}{2} - x, \frac{1}{2} + y, \frac{1}{2} - z, t\right) \times i\hat{\sigma}_y, \quad (2)$$

where the Bravais lattice vectors $\vec{R} = x\vec{a} + y\vec{b} + z\vec{c}$. We set the length of each lattice vector to unity, i.e., $|\vec{a}| = |\vec{b}| = |\vec{c}| = 1$. The Pauli matrices $\hat{\sigma} = (\hat{\sigma}_x, \hat{\sigma}_y, \hat{\sigma}_z)$ represent how spin transforms under the above symmetry operations. Note that another screw-axis operator \hat{S}_c is defined via $\hat{S}_c = \hat{S}_a * \hat{S}_b$.

In addition to these crystalline symmetries, the system also preserves time-reversal \hat{T} and inversion \hat{P} symmetries. The composite symmetry operator defined as the product of time-reversal and inversion operators ($\Theta \equiv \hat{T} * \hat{P}$) reverses the space-time and spin coordinates simultaneously, $\Theta : (x, y, z, t) \rightarrow (-x, -y, -z, -t) \times i\hat{\sigma}_y$. Since $\Theta^2 = -1$, it

*hykee@physics.utoronto.ca

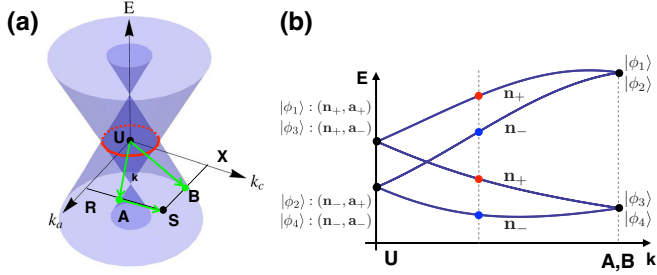


FIG. 1. The fourfold degenerate nodal line on the $k_b = \pi$ plane is shown as the red loop in (a). (b) shows the schematic band dispersion along the U - A and U - B lines, where A and B are arbitrary points on the R - S and X - S lines, respectively as depicted in (a). The Bloch states at the U point are labeled by \hat{G}_n and \hat{S}_a eigenvalues (n_{\pm}, a_{\pm}). All bands are doubly degenerate, and Kramers partners $\Theta|\phi_i\rangle$ have the same eigenvalues as $|\phi_i\rangle$ on these BZ boundaries. On the U - A and U - B lines, the Bloch states are labeled by n_{\pm} . $|\phi_2\rangle$ and $|\phi_3\rangle$ have to be exchanged along these paths enforcing the nodal ring FS.

enforces twofold degeneracy everywhere in the momentum space.

Note that the glide planes are found by taking the product of the above screw and inversion operators, i.e., \hat{b} -glide operator $\hat{G}_b = \hat{S}_a * \hat{P}$, n -glide $\hat{G}_n = \hat{S}_b * \hat{P}$, and mirror reflection at $z = 1/4$, $\hat{M}_c = \hat{S}_c * \hat{P}$. This corresponds to P_{bnm} lattice, but our proof below is general and applicable to other lattices with two orthogonal nonsymmorphic symmetries such as P_{bca} .

Now let us focus on the $k_b = \pi$ plane, which is invariant under \hat{G}_n operation. The Bloch states $|\phi_i\rangle$ on the plane carry \hat{n} -glide eigenvalues $n_{\pm} = \pm i e^{i \frac{k_a + k_c}{2}}$. Its Kramers partner, $\Theta|\phi_i\rangle$ is also an eigenstate of \hat{G}_n with the same \hat{n} -glide eigenvalue on this BZ boundary plane [38]. There are eight Bloch states, say $|\phi_i\rangle$ and $\Theta|\phi_i\rangle$, where $i = 1, \dots, 4$ for a single-orbital problem. In general, these Bloch states at a generic momentum point on the $k_b = \pi$ plane carry n_+ and n_- eigenvalues as shown in Fig. 1(b). At a time-reversal invariant momentum (TRIM) point $U = (k_a = 0, k_b = \pi, k_c = \pi)$, these Bloch states can be classified by eigenvalues of the \hat{n} glide as well as a screw axis operator \hat{S}_a along the \hat{a} axis. Since $(\hat{S}_a)^2 = -e^{i k_a}$, the eigenvalues $a_{\pm} = \pm i$ at the U point. Due to the presence of the \hat{b} -glide symmetry, two Bloch states $|\phi_1\rangle$ and $|\phi_3\rangle$, and $|\phi_2\rangle$ and $|\phi_4\rangle$ are in fact related under \hat{G}_b , i.e., $|\phi_3\rangle \propto \hat{G}_b|\phi_1\rangle$ and $|\phi_4\rangle \propto \hat{G}_b|\phi_2\rangle$ with the same \hat{n} glide but opposite screw eigenvalues as denoted in Fig. 1(b) at the U point. The fourfold degeneracy including a Kramers partner at the U point is protected by the \hat{n} glide and screw axis \hat{S}_a . On the other hand, along the R - S and X - S BZ boundary lines, where the Bloch states within each pair are related though \hat{G}_b and \hat{S}_a , respectively, $|\phi_1\rangle$ and $|\phi_2\rangle$, and $|\phi_3\rangle$ and $|\phi_4\rangle$ are degenerate with different \hat{n} -glide eigenvalues as shown in Fig. 2(c). Thus the two pairs of Bloch states at the U point must experience a partner switching between $|\phi_2\rangle$ and $|\phi_3\rangle$ when the bands evolve towards the BZ boundary line X - S or R - S on the $k_b = \pi$ plane. This also occurs for Kramers partner states. We refer to Appendix for proofs of Bloch states degeneracies at different BZ boundaries originated from the glide/screw symmetries. This enforces a fourfold degenerate nodal line on the $k_b = \pi$ plane with the U point as its center. The nodal

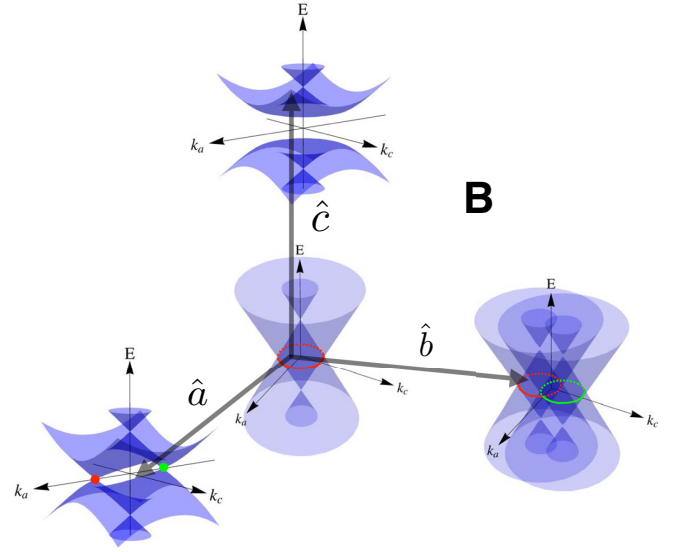


FIG. 2. Schematic plot to summarize how the direction of the magnetic field B perturbation affects the fourfold degenerate nodal-line FS. The grey axis is labeled the orientation of the magnetic field. All band dispersions are plotted on the $k_b = \pi$ plane. The nodal line (red solid/dashed line) FS, located at the origin, represents the case when TR symmetry is preserved. When $B \parallel \hat{c}$, the nodal-line FS is destroyed by having a bulk energy gap. Two fourfold nodal FSs emerge along the k_a direction after applying the B field parallel to the \hat{a} axis. On the other hand, the \hat{b} magnetic field splits the single nodal-ring FS into two Weyl rings.

line crossings hence are assured by the nonsymmorphic space group at a half-filling, which indicates the system should be a filling enforced semimetal [26,39].

III. TOPOLOGICAL SEMIMETALS WITHOUT TRS

In the above discussion, the TRS is crucial to ensure the fourfold degeneracy of nodal FS. Without TRS, the twofold degeneracy for each band is no longer guaranteed. However, possible fourfold degenerate nodal FSs can still be realized in the absence of TRS, as an antiunitary operator that leads to a double degeneracy like Kramers theorem. Below we will show how a nodal FS changes under magnetic field perturbations along three different directions and identify their topological nature without TRS. The two degenerate states could have the same eigenvalues of nonsymmorphic operations, leaving fourfold degenerate Dirac points on the BZ boundary line.

Applying a magnetic field along \hat{a} axis breaks the \hat{n} glide and mirror symmetry plane in addition to TRS. The schematic band structure are shown in Fig. 3. Under the magnetic field along the \hat{a} axis, each band remains doubly degenerate on the $k_b = \pi$ plane with a fourfold degenerate Dirac point crossing on the U - R high-symmetry line. An antiunitary operator Θ_n defined as the product of \hat{G}_n and Θ leads to a such degeneracy as shown below:

$$\Theta_n \equiv \hat{G}_n \Theta : (x, y, z, t) \rightarrow \left(\frac{1}{2} - x, \frac{1}{2} + y, \frac{1}{2} - z, -t \right) \times I . \quad (3)$$

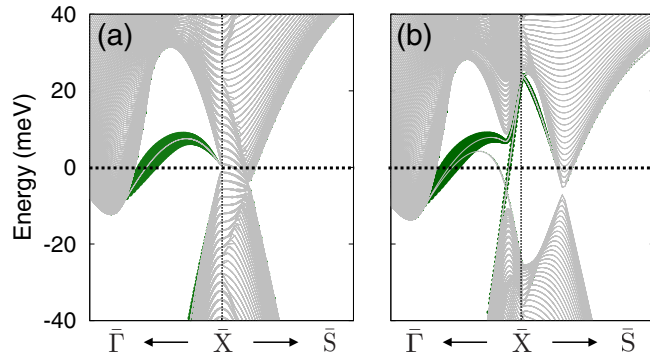


FIG. 3. (001) surface states in the presence of TRS. (a) shows the bands of the 40-layer-thick (001) slab geometry, with the surface weight of each Bloch state depicted as the size of the green symbol. (b) shows the bands with a sublattice potential that breaks mirror and \hat{n} -glide symmetries. The double helical surface states are represented by the green symbols where the size refers the weight.

While TRS and \hat{G}_n are broken, Θ_n is preserved. Furthermore, Θ_n symmetry is invariant on the $k_b = \pi$ plane with $(\Theta_n)^2 = e^{ik_b} = -1$ on this BZ boundary plane. Therefore, two orthogonal Bloch states $|\phi\rangle$ and $\Theta_n|\phi\rangle$ are degenerate, similar to Kramers doublets under TRS. In addition, the screw axis \hat{S}_a is also present.

Suppose that there is a Bloch state $|\phi\rangle$ on the U - R line with a_+ , the \hat{S}_a eigenvalue. Its Kramers partner $\Theta_n|\phi\rangle$ under the \hat{S}_a operation shows that $\hat{S}_a\Theta_n|\phi\rangle = a_+\Theta_n|\phi\rangle$. It carries the same screw \hat{S}_a eigenvalue with $|\phi\rangle$. Therefore a magnetic field along the \hat{a} direction will not lift the degeneracy along the U - R line. The fourfold degeneracy at the U point also remains intact due to the persistence of the screw axis along the \hat{a} direction. This pair of Dirac nodes, as demonstrated above, is thus protected by a screw axis \hat{S}_a and Θ_n . They can only be destroyed by annihilating them at BZ boundary, similar to the interlayer sublattice potential discussed in Ref. [24].

When the field is along the \hat{b} -axis, \hat{G}_b and TRS are both broken, and the fourfold degeneracy at the U point is lifted. However, the product of \hat{G}_b and \hat{T} is preserved on both the U - R and X - S BZ boundary lines:

$$\Theta_b \equiv \hat{G}_b\hat{T} : (x, y, z, t) \rightarrow \left(\frac{1}{2} - x, \frac{1}{2} + y, z, -t\right) \times i\hat{\sigma}_z. \quad (4)$$

The square of this antiunitary operator Θ_b is -1 on $k_b = \pi$, i.e., $\Theta_b^2 = e^{-ik_b} = -1$ implying that double degeneracy protected under the Θ_b operation occurs on the U - R and X - S lines. Θ_b operation on the Bloch state $|\phi_i\rangle$ with n_+ eigenvalues on the U - R line yields $\Theta_b|\phi_i\rangle$, which in fact possesses the same n -glide eigenvalue with $|\phi_i\rangle$. Thus the fourfold degenerate eigenstates on the U - R line are protected by the \hat{n} glide and Θ_b symmetry. The Bloch states at the R point still remain fourfold degenerate, which can be attributed to the preservation of the n glide. Meanwhile, since the screw rotation symmetry is broken by the magnetic field, a gap proportional to the strength of the magnetic field, appears at the U point. This degenerate Dirac nodes on the U - R line can be also understood as the intersect points between two nodal ring FSs as shown in Fig. 2. One fourfold degenerate nodal ring FS splits into two doubly

degenerate nodal ring (Weyl ring) FSs as they move upwards and downwards, respectively, along the U - X line under the presence of a magnetic field. The overlap between two nodal ring FSs makes the fourfold Dirac points, which eventually vanish when the magnetic field strength increases further.

Finally, we discuss the case with the magnetic field along the \hat{c} direction, where \hat{b} glide, \hat{n} glide, and TRS are all broken. The doubly degenerate states for each band on the $k_b = \pi$ plane can be explained by another emergent antiunitary operator Θ_n , which is defined as the product of \hat{n} -glide and Θ operator as in Eq. (3). Along the U - X line, the screw rotation symmetry along \hat{c} -axis $\hat{S}_c \equiv \hat{G}_b\hat{G}_n$ is invariant. The degenerate pair of $\Theta_n|\phi_i\rangle$ and $|\phi_i\rangle$ on the U - X line carry opposite screw eigenvalues. Therefore the fourfold degenerate points are avoided due to the hybridization, and completely gapped out the band degeneracy near the Fermi energy. A similar situation also occur on the U - R line where mirror symmetry is preserved and $[\hat{M}_c, \Theta_n] = 0$. It hence leads to gapped states on the U - R line. Besides, since the \hat{n} -glide symmetry is also broken, a generic momentum point on the $k_b = \pi$ plane should have a gap, and the system turns into a trivial band insulator.

IV. SURFACE STATES

Since the bulk nodal FSs are protected by the space-time inversion and nonsymmorphic symmetries, one can ask if there are nontrivial surface states associated with the bulk states. While the surface naturally breaks the inversion symmetry, surface states can possess nontrivial topology depending on the direction of surfaces. Given that the double degeneracy along the U - R and X - S lines are protected by the product of the b glide and TRS (Θ_b) without involving the inversion symmetry, a surface containing this glide plane could be potentially interesting. The (001) surface breaks the mirror and n glide, but preserves the b -glide symmetry. Thus we study the (001) surface states using a tight binding model derived for perovskite iridates AIrO_3 in Ref. [24].

As shown in Fig. 3(a), the (001) surface states perpendicular to the \hat{c} direction shows the surface bands across the Γ - X line. This is related to the Z_2 Dirac cone discussed in Ref. [34]. On the other hand, the surface states associated with the FS ring cannot be separated from the bulk spectrum across the X - S line. To gap out the bulk states but keeping the Θ_b invariance, one can introduce a sublattice potential [24,31]. The surface states are then double helical states named Riemann surface states [40] as shown in Fig. 3(b). TRS is essential for the existence of these surface states, and one then can ask what happens to them when the TRS is broken. When the field is along the a axis, the \hat{b} -glide plane is still preserved and furthermore the bulk states are gapped except two nodal points. As shown in Fig. 4, two Fermi arcs emerge from the bulk nodal points on each surface side: the double helical state splits into two Fermi arcs, and one appears on the top surface while the other appears on the bottom surface just like the Fermi arcs appearing from Dirac to Weyl FSs. Unlike the conventional Dirac point discovered so far, this nodal point accompanies two Fermi arcs on each side. The Chern number associated with the each nodal point is ± 2 .

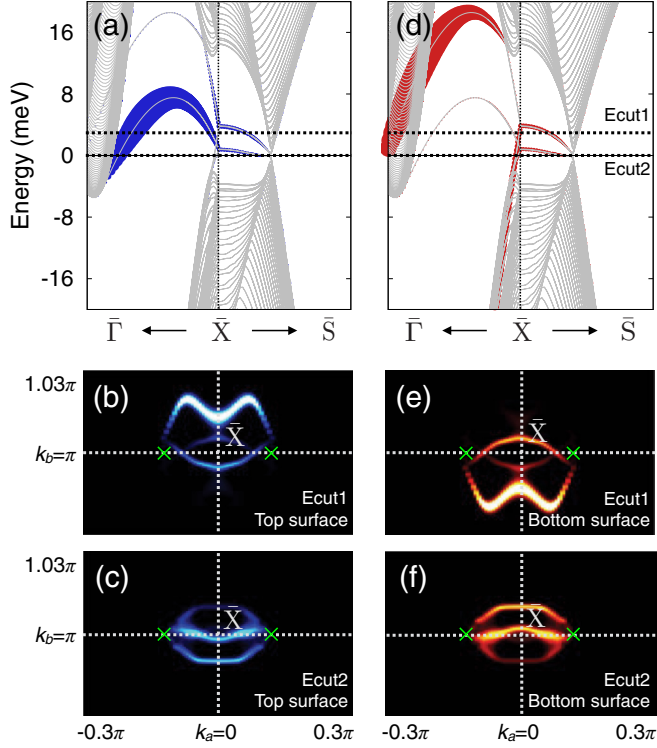


FIG. 4. (001) surface states in the presence of magnetic fields along the \hat{a} direction. (a)–(c) and (d)–(f) show the surface states on the top and bottom surfaces of the (001) slab geometry, respectively. (b), (e) and (c), (f) show the constant energy cut of the surface states in the momentum space at the energy $+2.5$ and 0 meV with respect to the Fermi level, respectively, as shown in (a) and (d). Green crosses in the constant energy plots mark the position of the surface-projected bulk Dirac points. These surface states represent two Fermi arcs from the fourfold degenerate Dirac points.

V. SUMMARY

In summary, we prove that the presence of fourfold degenerate nodal lines of FSs on the BZ boundary plane in 3D nonsymmorphic lattices is guaranteed, when there are two perpendicular nonsymmorphic symmetry operators, e.g., two perpendicular glide planes in addition to the space-time inversion symmetry. Our result is applicable for nonsymmorphic crystals with perpendicular glide/screw symmetry planes. Note that, in the experimentally relevant real materials such as SrIrO_3 , the presence of the hopping terms between the same sublattice explicitly break the chiral symmetry [34], and the nodal line hence acquires dispersion. While the amplitude of such hopping terms is tiny in SrIrO_3 [31,34], in other materials it can be a different case. However, this does not alter the main conclusion. We also show that fourfold Dirac FSs can survive even when TRS is absent. This is because the combination of nonsymmorphic and time-reversal symmetries is an antiunitary operator that leads to the double degeneracy like Kramers degeneracy. Using a tight-binding model derived for perovskite iridates, we also present the associated surface states with and without TRS. On the (001) surface where the product of the b glide and TRS is preserved, double helical surface states are found, but they are hidden under the bulk states. When the magnetic field is applied along

a certain direction that keeps the b -glide symmetry, double Fermi arcs associated with fourfold Dirac points appear, which indicates that these Dirac points are made of two Weyl points with the same topological charge. On the other hand, a pair of Weyl ring FSs emerges under the magnetic field along another direction. The current work suggests that materials with nonsymmorphic crystalline symmetries offer an excellent playground to explore rich topological phases.

ACKNOWLEDGMENTS

This work was supported by the Natural Sciences and Engineering Research Council of Canada and the Center for Quantum Materials at the University of Toronto.

APPENDIX: FOURFOLD DEGENERACY ENABLED THROUGH NONSYMMORPHIC SYMMETRIES WITH SPACE-TIME INVERSION SYMMETRY

Here, we provide a proof for the degeneracy between a pair of Bloch states related by nonsymmorphic symmetries when there are two perpendicular screw or glide symmetry operations. The two screw operators considered in the maintext are defined in Eq. (1) and (2), and, note that the screw axes are off-center from the inversion center, $(0,0,0)$. The axis for the \hat{S}_a screw operation is parallel to \hat{a} axis but it passes through $(0, b/4, 0)$, instead of $(0,0,0)$. The other screw rotation axis \hat{S}_b passes through $(a/4, 0, c/4)$, and is parallel to \hat{b} axis. Here, a , b , and c are the length of the Bravais lattice basis \hat{a} , \hat{b} , and \hat{c} , respectively. Note that, when squared, both \hat{S}_a and \hat{S}_b correctly reproduces the unit translations along the \hat{a} and \hat{b} directions, respectively. The space-time inversion symmetry defined as a product of TR and inversion operator, $\Theta = \hat{T} * \hat{P}$ is present: $\Theta : (x, y, z, t) \rightarrow (-x, -y, -z, -t) \times i\hat{\sigma}_y$. The c -axis screw operator is then given by $\hat{S}_c = \hat{S}_a * \hat{S}_b$ and the glide plane operators are also found by $\hat{G}_n = \hat{S}_b * \hat{P}$ and $\hat{G}_b = \hat{S}_a * \hat{P}$.

Since the degeneracy occurs on the BZ boundary plane, let us focus on the Bloch states on the $k_b = \pi$ plane. In this plane, the Bloch states are invariant under the n -glide operator \hat{G}_n , thus they can be classified by n -glide eigenvalues n_{\pm} . Given that $(\hat{G}_n)^2 = -e^{ik_a + ik_c}$, $n_{\pm} = \pm i e^{i\frac{k_a + k_c}{2}}$. All Bloch states on the $k_b = \pi$ plane carry one of these eigenvalues.

Now let us examine a particular high-symmetry U point ($k_a = 0, k_b = \pi, k_c = \pi$) on this BZ boundary plane. At the U point, the Bloch states are invariant under the screw \hat{S}_a operation in addition to G_n . Thus the Bloch states at the U point are denoted by both n -glide and a -axis screw eigenvalues. Since $(\hat{S}_a)^2 = -e^{ik_a}$, the eigenvalues of \hat{S}_a are $a_{\pm} = \pm i e^{i\frac{k_a}{2}}$ which is $\pm i$ at the U point. Taking the b -glide operation on a Bloch state $|\phi_1\rangle$, i.e., $\hat{G}_b|\phi_1\rangle$ generates another Bloch state with the same n -glide eigenvalue but different screw \hat{S}_a eigenvalue. These two are orthogonal and degenerate. The proof is shown as follows.

Let us consider a Bloch state $|\phi_1\rangle$ that carries n_+ and a_+ eigenvalues. Note that under \hat{G}_n and \hat{S}_a , $\hat{G}_b|\phi_1\rangle$ behave as

$$\hat{G}_n(\hat{G}_b|\phi_1\rangle) = \hat{G}_b(\hat{G}_n|\phi_1\rangle) = n_+ \hat{G}_b|\phi_1\rangle \quad (\text{A1})$$

$$\hat{S}_a(\hat{G}_b|\phi_1\rangle) = -\hat{G}_b(\hat{S}_a|\phi_1\rangle) = -a_+ \hat{G}_b|\phi_1\rangle = a_- \hat{G}_b|\phi_1\rangle, \quad (\text{A2})$$

TABLE I.

Symmetry	\hat{G}_b	\hat{G}_n	\hat{M}_c	Θ
\hat{G}_b	0	$\hat{G}_b \hat{G}_n = -e^{-ik_a+ik_b} \hat{G}_n \hat{G}_b$	$\{\hat{G}_b, \hat{M}_c\} = 0$	$\hat{G}_b \Theta = e^{-ik_a+ik_b} \Theta \hat{G}_b$
\hat{G}_n	$\hat{G}_n \hat{G}_b = -e^{ik_a-ik_b} \hat{G}_b \hat{G}_n$	0	$\hat{G}_n \hat{M}_c = -e^{ik_c} \hat{M}_c \hat{G}_n$	$\hat{G}_n \Theta = e^{ik_a-ik_b+ik_c} \Theta \hat{G}_n$
\hat{M}_c	$\{\hat{G}_b, \hat{M}_c\} = 0$	$\hat{M}_c \hat{G}_n = -e^{-ik_c} \hat{G}_n \hat{M}_c$	0	$\hat{M}_c \Theta = e^{-ik_c} \Theta \hat{M}_c$
Θ	$\hat{G}_b \Theta = e^{-ik_a+ik_b} \Theta \hat{G}_b$	$\hat{G}_n \Theta = e^{ik_a-ik_b+ik_c} \Theta \hat{G}_n$	$\hat{M}_c \Theta = e^{-ik_c} \Theta \hat{M}_c$	0

where we used the commutation relations given in Table I: \hat{G}_b commutes with \hat{G}_n but anticommutes with \hat{S}_a . We also used $a_- = -a_+$. This suggests that $\hat{G}_b|\phi_1\rangle$ is also an eigenstate of both \hat{G}_n and \hat{S}_a operators with n_+ and a_- eigenvalues, respectively. As mentioned in the main text, we denote this Bloch state $|\phi_3\rangle$, which is proportional to $\hat{G}_b|\phi_1\rangle$ up to a $U(1)$ phase factor. Furthermore, the inner product of these two Bloch states is given by

$$\begin{aligned} \langle \phi_1 | \hat{G}_b | \phi_1 \rangle &= -\langle \phi_1 | (\hat{S}_a)^2 \hat{G}_b | \phi_1 \rangle = -(-\hat{S}_a | \phi_1 \rangle)^\dagger \hat{S}_a \hat{G}_b | \phi_1 \rangle \\ &= -\langle \phi_1 | \hat{G}_b | \phi_1 \rangle, \end{aligned} \quad (\text{A3})$$

where $(\hat{S}_a)^2 = -1$ at the U point is used. This implies $\langle \phi_1 | \hat{G}_b | \phi_1 \rangle = 0$ and thus $|\phi_1\rangle$ and $|\phi_3\rangle$ are orthogonal. Since \hat{G}_b commutes with the Hamiltonian, we proved that $|\phi_1\rangle$ and $|\phi_3\rangle$ are degenerate at the U point. Following a similar argument, another pair of Bloch states $(|\phi_2\rangle, |\phi_4\rangle)$ are degenerate where $|\phi_4\rangle \propto \hat{G}_b |\phi_2\rangle$. Thus taking into account their Kramers partners [38], two sets of four Bloch states— $(|\phi_1\rangle, |\phi_3\rangle, \Theta|\phi_1\rangle, \Theta|\phi_3\rangle)$ and $(|\phi_2\rangle, |\phi_4\rangle, \Theta|\phi_2\rangle, \Theta|\phi_4\rangle)$ —are degenerate at the U point.

How do these Bloch states evolve as they move to a generic point on the R - S and X - S BZ boundary line in the $k_b = \pi$ BZ plane? As discussed in the maintext, along the R - S and X - S BZ boundary line, $|\phi_1\rangle$ and $|\phi_2\rangle$ ($|\phi_3\rangle$ and $|\phi_4\rangle$) are degenerate and related by \hat{G}_b (\hat{S}_a). To prove our statement, let us consider an arbitrary point on the R - S line ($k_a = \pi, k_b = \pi$), where the Bloch states are invariant under the b - and n -glide operation. Using the commutation relation given in Table I, i.e., $\hat{G}_b \hat{G}_n = -e^{-i(k_a=\pi)+i(k_b=\pi)} \hat{G}_n \hat{G}_b = -\hat{G}_n \hat{G}_b$, the Bloch state $\hat{G}_b|\phi_1\rangle$ on the R - S line under an n -glide operator \hat{G}_n

carries an n_- eigenvalue as shown below:

$$\hat{G}_n(\hat{G}_b|\phi_1\rangle) = -\hat{G}_b(\hat{G}_n|\phi_1\rangle) = -n_+ \hat{G}_b|\phi_1\rangle = n_- \hat{G}_b|\phi_1\rangle. \quad (\text{A4})$$

Thus $\hat{G}_b|\phi_1\rangle$ with an opposite n -glide eigenvalue becomes degenerate with $|\phi_1\rangle$ along the R - S line, as \hat{G}_b commutes with the Hamiltonian on the R - S line. Using a similar process including orthogonality, $\langle \phi_1 | \hat{G}_b | \phi_1 \rangle = \langle \phi_1 | \hat{G}_b \Theta | \phi_1 \rangle = 0$, we showed that two pairs of four Bloch states, $(|\phi_1\rangle, |\phi_2\rangle, \Theta|\phi_1\rangle, \Theta|\phi_2\rangle)$ and $(|\phi_3\rangle, |\phi_4\rangle, \Theta|\phi_3\rangle, \Theta|\phi_4\rangle)$ including a Kramers doublet are degenerate on the R - S line. Hence $|\phi_2\rangle$ and $|\phi_3\rangle$ with opposite and same n -glide eigenvalue at the U point exchange their degenerate partner, as they move from U to any other point along the R - S line as shown in Fig. 1(b) in the main text. The energy level crossing should occur somewhere in between, unless these nonsymmorphic symmetries are broken.

Similarly, a band crossing should occur somewhere between the U point to any point on the X - S BZ boundary line ($k_b = \pi, k_c = 0$), where the Bloch states are invariant under \hat{G}_n and \hat{S}_a operations. Since they anticommute, i.e., $\hat{S}_a \hat{G}_n = -e^{-i(k_c=0)} \hat{G}_n \hat{S}_a = -\hat{G}_n \hat{S}_a$, another Bloch state $\hat{S}_a|\phi_1\rangle$ generated by taking \hat{S}_a on $|\phi_1\rangle$ has the opposite n -glide eigenvalue from $|\phi_1\rangle$. Since $|\phi_2\rangle \propto \hat{S}_a|\phi_1\rangle$ on the X - S line, and \hat{S}_a commutes with the Hamiltonian, we find $(|\phi_1\rangle, |\phi_2\rangle, \Theta|\phi_1\rangle, \Theta|\phi_2\rangle)$ and $(|\phi_3\rangle, |\phi_4\rangle, \Theta|\phi_3\rangle, \Theta|\phi_4\rangle)$ are degenerate on the X - S line.

In summary, we prove that two pairs of Bloch states denoted as $(|\phi_1\rangle, |\phi_3\rangle)$ and $(|\phi_2\rangle, |\phi_4\rangle)$ at the U point must switch a degenerate partner when the bands move from the U point towards the BZ boundary line of the X - S and R - S lines, which results in a ring of fourfold degenerate FS on the $k_b = \pi$ BZ plane.

The commutation table among b -glide, n -glide, mirror, and Θ operators established in the end is used to demonstrate the mathematical proof provided in the above discussion.

- | | |
|--|--|
| <p>[1] C. L. Kane and E. J. Mele, <i>Phys. Rev. Lett.</i> 95, 146802 (2005).
 [2] B. A. Bernevig and S.-C. Zhang, <i>Phys. Rev. Lett.</i> 96, 106802 (2006).
 [3] B. A. Bernevig, L. H. Taylor, and S.-C. Zhang, <i>Science</i> 314, 1757 (2006).
 [4] L. Fu and C. L. Kane, <i>Phys. Rev. B</i> 76, 045302 (2007).
 [5] L. Fu, C. L. Kane, and E. J. Mele, <i>Phys. Rev. Lett.</i> 98, 106803 (2007).
 [6] J. E. Moore and L. Balents, <i>Phys. Rev. B</i> 75, 121306(R) (2007).
 [7] M. König, S. Wiedmann, C. Bruce, A. Roth, H. Buhmann, L. Molenkamp, X. L. Qi, and S.-C. Zhang, <i>Science</i> 318, 766 (2007).</p> | <p>[8] D. Hsieh, D. Qian, L. Wray, Y. Xia, Y. S. Hor, R. J. Cava, and M. Z. Hasan, <i>Nature (London)</i> 452, 970 (2008).
 [9] D. Hsieh, Y. Xia, L. Wray, D. Qian, A. Pal, J. H. Dil, J. Osterwalder, F. Meier, G. Bihlmayer, C. L. Kane, Y. S. Hor, R. J. Cava, and M. Z. Hasan, <i>Science</i> 323, 919 (2009).
 [10] M. Z. Hasan and C. L. Kane, <i>Rev. Mod. Phys.</i> 82, 3045 (2010).
 [11] X. L. Qi and S.-C. Zhang, <i>Rev. Mod. Phys.</i> 83, 1057 (2011).
 [12] Z. K. Liu, B. Zhou, Y. Zhang, Z. J. Wang, H. M. Weng, D. Prabhakaran, S.-K. Mo, Z. X. Shen, Z. Fang, X. Dai, Z. Hussain, and Y. L. Chen, <i>Science</i> 343, 864 (2014).</p> |
|--|--|

- [13] S. Borisenko, Q. Gibson, D. Evtushinsky, V. Zabolotnyy, B. Buchner, and R. J. Cava, *Phys. Rev. Lett.* **113**, 027603 (2014).
- [14] S.-Y. Xu, I. Belopolski, N. Alidoust, M. Neupane, Guang Bian, Chenglong Zhang, Raman Sankar, Guoqing Chang, Zhujun Yuan, Chi-Cheng Lee, Shin-Ming Huang, Hao Zheng, Jie Ma, Daniel S. Sanchez, BaoKai Wang, Arun Bansil, Fangcheng Chou, Pavel P. Shibayev, Hsin Lin, Shuang Jia, and M. Zahid Hasan, *Science* **349**, 613 (2015).
- [15] B. Q. Lv, H.M. Weng, B.B. Fu, X.P. Wang, H. Miao, J. Ma, P. Richard, X.C. Huang, L.X. Zhao, G.F. Chen, Z. Fang, X. Dai, T. Qian, and H. Ding, *Phys. Rev. X* **5**, 031013 (2015).
- [16] G. E. Volovik, *Lect. Notes Phys.* **718**, 31 (2007).
- [17] S. Murakami, *New J. Phys.* **9**, 356 (2007).
- [18] A. A. Burkov and Leon Balents, *Phys. Rev. Lett.* **107**, 127205 (2011).
- [19] X. Wan, A. M. Turner, A. Vishwanath, and S. Y. Savrasov, *Phys. Rev. B* **83**, 205101 (2011).
- [20] K. Y. Yang, Y. M. Lu, and Y. Ran, *Phys. Rev. B* **84**, 075129 (2011).
- [21] S. M. Young, S. Zaheer, J. C. Y. Teo, C. L. Kane, E. J. Mele, and A. M. Rappe, *Phys. Rev. Lett.* **108**, 140405 (2012).
- [22] Z. Wang, Y. Sun, X. Q. Chen, C. Franchini, G. Xu, H. Weng, X. Dai, and Z. Fang, *Phys. Rev. B* **85**, 195320 (2012).
- [23] Z. Wang, H. Weng, Q. Wu, X. Dai, and Z. Fang, *Phys. Rev. B* **88**, 125427 (2013).
- [24] J. M. Carter, V. V. Shankar, M. A. Zeb, and H.-Y. Kee, *Phys. Rev. B* **85**, 115105 (2012).
- [25] A. A. Burkov, M. D. Hook, and L. Balents, *Phys. Rev. B* **84**, 235126 (2011).
- [26] S. A. Parameswaran, A. M. Turner, D. P. Arovas, and A. Vishwanath, *Nat. Phys.* **9**, 299 (2013).
- [27] C.-K. Chiu and A. P. Schnyder, *Phys. Rev. B* **90**, 205136 (2014).
- [28] M. Phillips and V. Aji, *Phys. Rev. B* **90**, 115111 (2014).
- [29] H. Weng, Y. Liang, Q. Xu, R. Yu, Z. Fang, X. Dai, and Y. Kawazoe, *Phys. Rev. B* **92**, 045108 (2015).
- [30] Y. Kim, B. J. Wieder, C. L. Kane, and A. M. Rappe, *Phys. Rev. Lett.* **115**, 036806 (2015).
- [31] Y. Chen, Y.-M. Lu, and H.-Y. Kee, *Nat. Commun.* **6**, 6593 (2015).
- [32] L. S. Xie, L. M. Schoop, E. M. Seibel, Q. D. Gibson, W. Xie, and R. J. Cava, *APL Mater.* **3**, 083602 (2015).
- [33] R. Yu, H. Weng, Z. Fang, X. Dai, and X. Hu, *Phys. Rev. Lett.* **115**, 036807 (2015).
- [34] H.-S. Kim, Y. Chen, and H.-Y. Kee, *Phys. Rev. B* **91**, 235103 (2015).
- [35] C.-K. Chiu, J. C. Teo, A. P. Schnyder, and S. Ryu, [arXiv:1505.03535](https://arxiv.org/abs/1505.03535) [Rev. Mod. Phys. (to be published)].
- [36] G. Bian *et al.*, *Nat. Commun.* **7**, 10556 (2016).
- [37] M. Zeng, C. Fang, G. Chang, Y.-A. Chen, T. Hsieh, A. Bansil, H. Lin, and L. Fu, [arXiv:1504.03492](https://arxiv.org/abs/1504.03492).
- [38] C. Fang, Y. Chen, H.-Y. Kee, and L. Fu, *Phys. Rev. B* **92**, 081201(R) (2015).
- [39] H. Watanabe, H. C. Po, A. Vishwanath, and M. P. Zaletel, *Proc. Natl. Acad. Sci. USA* **112**, 14551 (2015).
- [40] C. Fang, L. Liu, J. Liu, and L. Fu, [arXiv:1512.01552](https://arxiv.org/abs/1512.01552).